J Electr Eng Technol.2018; 13(6): 2329-2334
http://doi.org/10.5370/JEET.2018.13.6.2329

ISSN(Print) 1975-0102
ISSN(Online) 2093-7423

Effect of Axial-Layered Permanent-Magnet on Operating Temperature in Outer Rotor Machine

Phuong Thi Luu*, Ji-Young Lee†,*, Ji-Won Kim*,*, Yon-Do Chun*,*** and Hong-Seok Oh*****

Abstract – This paper discusses the thermal effect of the number of permanent-magnet (PM) layers in an outer rotor machine. Depending on the number of axial-layer of PM, the operating temperature is compared analytically and experimentally. The electromagnetic analysis is performed using 3-dimensional time varying finite element method to get the heat sources depending on axial-layered PM models. Then thermal analysis is conducted using the lumped-parameter-thermal-network method for each case. Two outer rotor machines, which have the different number of axial-layer of PM, are manufactured and tested to validate the analysis results.

Keywords: Axial-layered permanent magnet, Eddy current loss, Lumped-parameter-thermal-network.

1. Introduction

The permanent-magnet (PM) synchronous motors using NdFeB magnet with high torque density and high efficiency are strong candidates in many industrial applications. However, NdFeB is known as a good electric conductive material, so that the eddy current loss which is induced in the PM should not be neglected, especially in high-speed application. The eddy current loss rise leads to many undesirable problems such as reducing the power efficiency, reducing the torque, and in particularly causing the irreversible demagnetization in the magnet. Among various ways in an effort to reduce the eddy current loss, dividing the magnets into small parts is one of the most effective ways and it has been empirically proven [1-5].

Along with the increase in the eddy current losses is the increase in motor temperature. Commonly, thermal analysis is neglected or in other words, it draws less attention more than electromagnetic analysis in the motor design. However, the dependence of the permanent magnet characteristic on the temperature rise, for example the operating point of NdFeB magnet rises as the temperature increase lead to irreversible demagnetization, makes the thermal estimation problem become extremely important issue for PMSMs.

There are a large number of publishes presented the effectiveness of the layered PM on the eddy current loss [1-6], but no significant studies that show their effect on thermal behavior of motor. In order to evaluate the impact of magnet layer number from the thermal point of view, a comparative thermal analysis on the outer-rotor type PMSMs with different number of axial-layered PM is investigated in detail in this paper.

To implement the thermal analysis accurately and fairly, the motors under study have identical stator and share the same key rotor parameters and magnet volume. Firstly, the basic loss components including eddy current loss of PM (PM loss), and the eddy and hysteresis loss of the core (iron loss) are calculated by electromagnetic analysis using time-varying finite element method (FEM). Then, these loss values will be applied to the lumped-parameter-thermal-network (LPTN) to analyze motor temperature. Finally, to examine the validity of the analysis, the experimental is carried out for both single- and multi-layered PM models.

2. Model Specifications and Loss Analysis

2.1 Model specifications

The main purpose of this work is to analyze the effectiveness of the axial-layered PM on the thermal behavior of motors to suggest the suitable magnet configuration rather than to estimate the temperature of motor to optimize the design to satisfy the limitation. In order to ensure fairness in comparison, there are some assumptions are given as below:

1) All studied motors should keep the same main critical parameters of stator, rotor, axial length and cooling system. Only the number of axial-layered of PM will be changed.
2) All studied motors have the same grade and volume of PM materials, iron core, and copper material.
3) To simplify the complexity of the electromagnetic

† Corresponding Author: Electric Motor Research Center, Korea Electrotechnology Research Institute, Korea. (jylee@keri.re.kr)
* Dept. of Energy and Power Conversion Engineering, Korea University of Science and Technology, Korea.
** Electric Motor Research Center, Korea Electrotechnology Research Institute, Korea.
*** Star Group Industry Company (SGI), Korea.
Received: October 30, 2017; Accepted: July 6, 2018

Table 1. Main design parameters of the outer rotor machine

Output Characteristic	Output power	30 kW
	Max speed	2000 rpm
	Max torque	143.2 Nm
Dimensions	Rotor outer diameter	279 mm
	Rotor inner diameter	259 mm
	Stator outer diameter	256 mm
	Stator inner diameter	194 mm
	Stacking length	50 mm
	PM thickness	4 mm
	Number of stator slot/ rotor pole	18/24
Material	Magnet	NdFeB-38EH
	Core material	35PN250

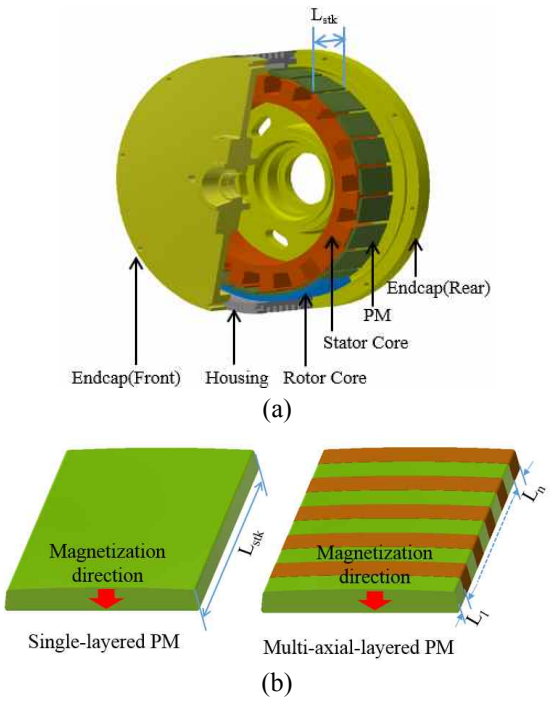

Fig. 1. (a) Overview of motor and (b) configuration of one magnet pole according to the usage of layer

calculation and thermal analysis, we only consider motors under no load condition operation at a rotation speed of 2000 rpm. In other words, the copper loss in the winding is not considered in this paper.

4) Practically, each PM layer is electrically isolated from each other by a small layer of insulation. The gap length of this insulation is only 0.03mm. Compare to the axial length of PM, which is 50mm, it is too small. Therefore, to simplify the analysis modeling these small gaps between PM layers are not considered and instead of that, the insulating boundary is used to separate electrically magnet layers from each other.

The main design specifications of the studied models are shown in Table 1, and the motor construction is schematically shown in Fig. 1(a). The studied motor adopts an outer rotor topology with a high number of poles to maximize the torque radius and gives a great interior space for the mechanical parts, such as bearings and supporting components [7]. With the same 50mm of stacking length (L_{stk}), the motors with up to ten axial-layered PM are investigated. Fig. 1(b) shows the PM configurations with single- and multi-layered PM, each layer has a uniform length in the axial direction (L_1=L_2=…=L_n).

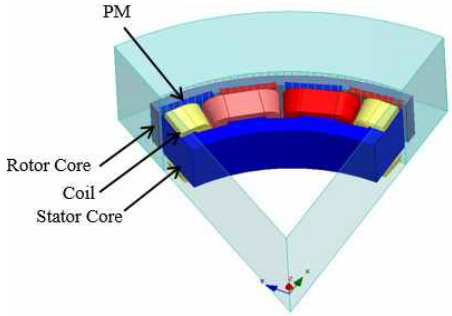

Fig.2. 1/6 periodic 3-D FEM model

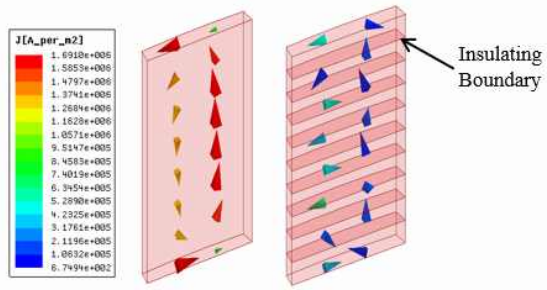

Fig. 3. Eddy current vector distribution in one pole for (a) single-layer of PM and (b) 10 axial-layers of PM

2.2 Loss analysis results

The two majorities of the motor losses considered under this study are the iron loss and PM loss. These two basic losses depend on the number of axial-layered PM are calculated by three-dimensional (3-D) electromagnetic FEM. All the related theories and Maxwell's electro-magnetic equation are presented in [8].

Since the model has a fractional slot per pole configuration, thus 1/6 periodic of the machine is modelled in 3-D FEM, as shown in Fig. 2. It consists of a stator core, three-phase coils, and a rotating part that includes the rotor core and PMs.

Fig. 3 shows the example of eddy current vector distribution in one pole for single-layer of PM and 10 axial-layers of PM. It could be seen that along with divided magnet, the eddy current paths are also divided into smaller loops, which lead to increase the effective resistance and consequently decrease the PM loss. The PM loss and iron loss at the different number of axial-layer of PM can be obtained as shown in Fig. 4. These results show that the PM loss decreases dramatically with the increase of number of axial-layered PM. It can be seen that the

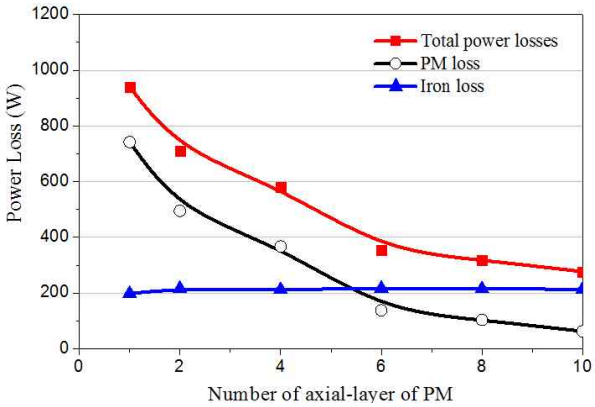

Fig. 4. The power loss depends on the number of axial-layer of PM

PM loss value in the case of 10 axial-layers of magnet is declined about 91.5% in comparison with in the case of single-layer of magnet. The iron loss also changes as a result of magnet layer, because the eddy currents have a little influence on the total flux through the rotor iron [5].

3. Thermal Parameters Computation Methods

3.1 LPTN method

LPTN models have been successfully utilized and verified on numerous machine types. Such a large number of published studies has proven its advantages in such thermal models. Therefore, in this study, the LPTN method using commercial software, Motor-CAD, as shown in [9], is used for thermal analysis of outer-rotor PMSM with the difference in the number of axial magnet layer.

As is well known, in a thermal network it is possible to lump together components that have similar temperatures and to represent each as a single node in the network. Lumped thermal parameters analysis involves the determination of thermal resistances, including conduction, radiation, and convection thermal resistance; those are used to separate nodes. Those main thermal parameters are calculated by program considering cooling system as summarized in hereafter Eqs. (1)~(3) [10].

$$R_c = \frac{L}{kA} \tag{1}$$

$$R_r = \frac{1}{h_R A} \tag{2}$$

$$R_{conv} = \frac{1}{h_C A} \tag{3}$$

where R_c , R_r , R_{conv} stand for conduction, radiation, and convection thermal resistance, respectively; L is the path length, in meters; A is the path area, in square meters; k is the thermal conductivity of the material, in watt per meter degree Celsius; h_R and h_c are radiation- and convection-heat-transfer coefficient.

3.2 Critical thermal parameter computation methods

a) Forced convection-heat-transfer coefficient in air gap

Forced convection is considered for thermal transfer in the air gap because of air flow by rotor rotating. The value Taylor (Ta) number is used to determine whether the air flow is laminar, vortex, or turbulent. The flow is assumed to be fully laminar if $Ta < 41$. The flow is assumed to be fully turbulent if $Ta > 100$. If $41 < Ta < 100$, the flow is vortex. Ta can be calculated by using equation (4):

$$Ta = \mathrm{Re}(l_g / R_r)^{0.5} \tag{4}$$

where l_g is the air gap radial length, R_r is the rotor inner radius, and Re is the Reynold number based on effective velocity as shown below:

$$\mathrm{Re} = v_e l_g / \mu \tag{5}$$

$$v_e = \sqrt{v_a^2 + (1/4)v_r^2} \tag{6}$$

with v_e is the effective velocity, v_a is the axial velocity of flow, and v_r is the peripheral velocity of the rotor. For small gaps compared with the radius, this means rotational velocity is simply one-half the rotor velocity [11].

In our studied model, Ta = 196.4 > 100 the flow becomes fully turbulent, so the corresponding Nu can be calculated by (7) [12]:

$$Nu = 0.386 Ta^{0.5} \mathrm{Pr}^{0.27} \tag{7}$$

Coefficient of convective-heat-transfer is obtained by

$$h_C = \frac{Nu \times k}{2 \times l_g} \tag{8}$$

b) Forced convection-heat-transfer in housing outer surface

The model under studied case is outer rotor type PMSM. Therefore, the housing geometry is considered as a rotating cylinder to define the heat transfer by convection between housing outer surface and a surrounding air. The average Nu (Nusselt) number for a horizontal cylinder rotating in the air can be derived from experimental data with the Re (Reynolds) and Gr (Grashof) number based on the diameter of the cylinder and rotating speed, as expressed in equation (11) [13].

$$\mathrm{Re} = \rho \pi D^3 \omega / \mu \tag{9}$$

$$Gr = \rho^2 \beta g (T_s - T_\infty) D^3 / \mu^2 \tag{10}$$

$$Nu = \frac{hD}{k} = 0.11(0.5\,\mathrm{Re}_\omega^2 + Gr\,\mathrm{Pr})^{0.35} \tag{11}$$

where D is the housing outer diameter, in meters; ρ is the air density, in kg/m^3; ω is the rotation speed, in rad/s; μ is the air dynamic viscosity, in m^2/s; β is the air expansion coefficient, in 1/^{o}C; T_s and T_∞ are the housing outer surface temperature and ambient temperature, respectively; Pr is the Prandtl number.

4. Thermal Analysis Results and Experimental Validation

In order to study the thermal behavior of the machine depending on the number of axial-layered of PM, the comparative thermal analysis is implemented on the studied PM motors at the speed of 2000 rpm under no-load condition. Table 2 shows the thermal conductivity of important materials and heat-transfer-coefficients of the main parts which are determined by using the theory presented in section 3.

Fig. 5 shows the thermal resistance network schematic of single-layer PM motor, in which all the components are put together to present the heat transfer in the machine. By solving this schematic, the steady state or transient thermal performance is computed. All the thermal resistance is determined by commercial software using theory of section 3. Then the temperature at all nodes in the thermal network is calculated.

Table 2. Constants and coefficients for thermal analysis

Material	Thermal Conductivity	Note
35PN250	30 W/m/^{o}C	Rotor and Stator Core
Copper	401 W/m/^{o}C	Winding
N38EH	6.4 W/m/^{o}C	Permanent Magnet
Epoxy resin	0.22 W/m/^{o}C	Molding of winding
Aluminum	167 W/m/^{o}C	Housing
Heat transfer coefficient		
Housing outside	306.9 W/m^2/^{o}C	Convection+Radiation
Air gap	51.2 W/m^2/^{o}C	Convection

Fig. 6 shows the comparison of temperature variation in major parts versus the number of axial-layered PM from the thermal analysis results. With the increasing of the axial-layered PM number, the temperature in the all major parts of the motor is remarkably decreased due to decreasing of PM loss. A temperature of stator is higher than that of winding because we consider the no-load condition in this study. A temperature of the magnet and rotor is quite small compared with stator and winding, because forced convection is considered in both air gap and

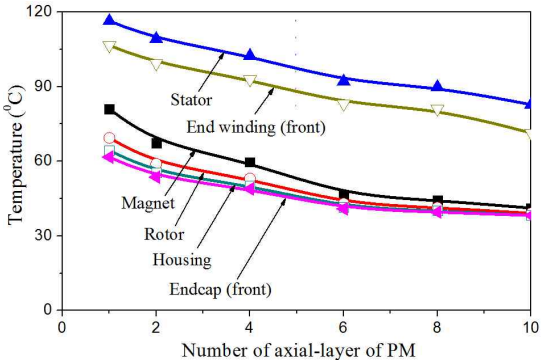

Fig. 6. Operating temperature variation on the main parts according to the number of axial- layered PM

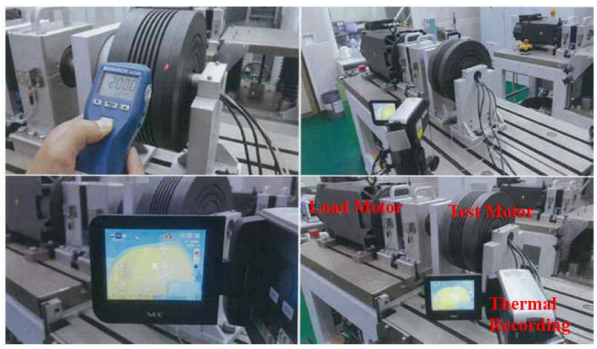

Fig. 7. Configuration of experimental system

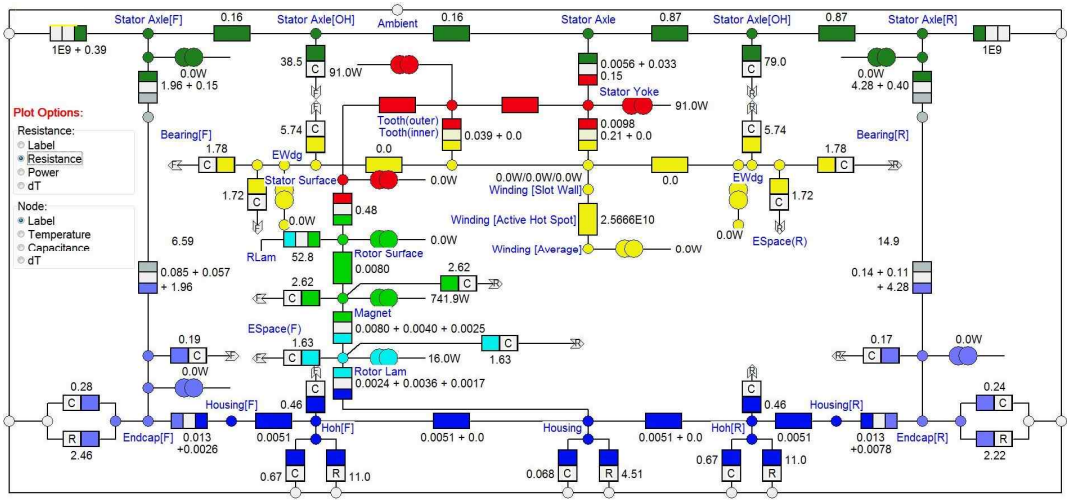

Fig. 5. Thermal resistance network schematic of single-layered magnet motor

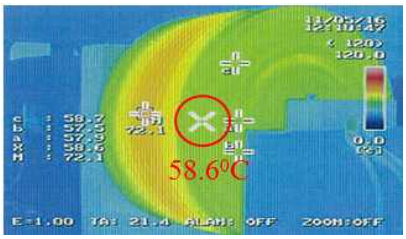

(a) motor with single-layer PM

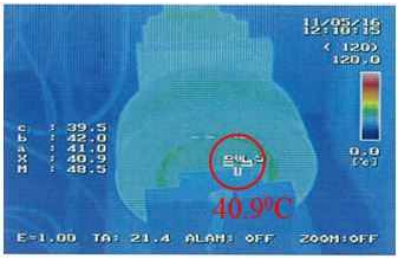

(b) motor with 10 axial-layers PM

Fig. 8. The thermal distribution on the two motors operated in open-circuit at 2000 rpm

outer surface housing due to rotating speed of 2000 rpm.

After analyzing the effect of axial-layered PM on reducing the PM loss and operating temperature in motors, two prototypes with single- and ten-axial-layered of PM are fabricated. The thermal test is conducted within 60 minutes for validating the thermal analysis results. The thermal testing device records the operating temperature on the front endcap of the two motors, as shown in Fig. 7. The temperature in the front of the endcap of single-layered PM motor is 58.6°C, meanwhile that figure is 40.9°C in the case of 10 axial-layers of PM motor, as shown in Fig. 8. The accuracy of test results up to 98.8% for single-magnet layer motor and 93.4% for 10 axial-layers of PM motor compared to the analysis results. According to the experimental results, the thermal analysis using LPTN method confirmed its excellent accuracy.

5. Conclusion

The accuracy of analysis results were examined and confirmed by comparing it with experimental results. Therefore, the results of the simulation can be used to analyze and then suggest which number of axial-layer of PM is proper in this study. Fig. 9 shows the operating temperature and total power losses variation with the number of axial-layered PM increasing from 1 to 10. These values were normalized on the basis of the operating temperature and total power losses when the number of layered PM is one. Overall, both of the operating temperature and total power losses are reduced when the number of axial-layer of PM increases. It can be clearly seen from Fig. 9 that the rate of change according to the number of axial-layered PM can be divided into 2 different groups. When the number of axial-layered PM increase

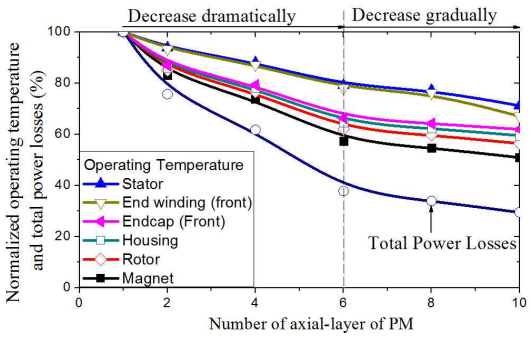

Fig. 9. Comparison of operating temperature and power loss between multi-layered PM and single-layer PM

from 1 to 6 layers, both operating temperature and total power losses significantly decrease by approximately 30~43% and 62%, respectively. While these values decrease slightly when the number of axial-layered PM increase in the range from 6 to 10 layers, which are under 10%. Therefore, after considering the analysis results and practical issues when splitting the magnets, such as the manufacturing cost, mechanical strength of magnets, outer-rotor PMSM with 6-axial-layers of PM configuration is proper for the PM axial length in this study.

Acknowledgements

This research was supported by Korea Electro-technology Research Institute (KERI) Primary research program through the National Research Council of Science & Technology (NST) funded by the Ministry of Science and ICT (MSIT) (No. 18-12-N0101-27).

References

[1] Jason D. Ede, Kais Atallah, Geraint W. Jewell, Jiabin B. Wang, and David Howe, "Effect of Axial Segmentation of Permanent Magnets on Rotor Loss in Modular Permanent-Magnet Brushless Machines," *IEEE Trans. Industry Applications*, vol.43, no.5, pp. 1207-1213, Sep. 2007.

[2] J. Klötzl, M. Pyc, and D. Gerling, "Permanent Magnet Loss Reduction in PM Machines using Analytical and FEM Calculation," *International Symposium on Power Electronics*, Electrical Drives, pp. 88-89, 2010.

[3] Shuangxia Niu, S. L.Ho, W.N. Fu, and Jianguo Zhu, "Eddy Current Reduction in High-Speed Machines and Eddy Current Loss Analysis With Multislice Time-Stepping Finite-Element Method," *IEEE Trans. on Magnetics*, vol. 48, no. 2, pp. 1007-1010, Feb. 2012.

[4] Wan-Ying Huang, Adel Bettayeb, Robert Kaczmarek, and Jean-Claude Vannier, "Optimization of Magnet Segmentation for Reduction of Eddy-Current Losses

in Permanent Magnet Synchronous Machine," *IEEE Trans. Energy Conversion*, vol. 25, no. 2, pp. 381-387, June 2010.
[5] Peter Sergeant and Alex Van den Bossche, "Segmentation of Magnets to Reduce Losses in Permanent-Magnet Synchronous Machines," IEEE *Trans. on Magnetics*, vol.48, no. 11, pp. 4409-4412, Nov. 2008.
[6] Mehran Mirzaei, Andreas Binder, Bogdan Funieru, and Marko Susic, "Analytical Calculations of Induced Eddy Currents Losses in the Magnets of Surface Mounted PM Machines With Consideration of Circumferential and Axial Segmentation Effects," *IEEE Trans. on Magnetics*, vol. 48, no. 12, pp. 4831-4841, Dec. 2012.
[7] Shi-Uk Chung, Seok-Hwan Moon, Dong-Jun Kim,, and Jong-Moo Kim, "Development of a 20-Pole-24-Slot SPMSM With Consequent Pole Rotor for In-Wheel Direct Drive," *IEEE Trans. Industrial Electronics*, vol. 63, no. 1, pp. 302-309, Jan. 2016.
[8] "Theory reference," Ansys Help System Ansys Inc., 2009.
[9] Motor-CAD. [Online]. Available: www.motor-design.com.
[10] Aldo Boglietti, Andrea Cavagnino, David Staton, Martin Shanel, Markus Mueller, and Carlos Mejuto, "Evolution and Modern Approaches for Thermal Analysis of Electrical Machines," *IEEE Trans. Industrial Electronics*, vol. 56, no. 3, pp. 249-255, March 2010.
[11] Sebastien Poncet, Sofia Haddadi, Stephane Viazzo, "Numerical Modeling of Fluid Flow and Heat Transfer in a Narrow Taylor-Couette-Poiseuille System," *International Journal of Heat and Fluid Flow*, vol. 32, no. 1, pp. 128-144, 2011.
[12] David A. Staton and Andrea Cavagnino, "Convection Heat Transfer and Flow Calculations Suitable for Analytical Modelling of Electric Machines," *IEEE Trans. Industrial Electronics*, vol. 55, no. 10, pp. 3509-3516, 2008.
[13] Frank Kreith, Raj M. Manglik, Mark S. Bohn, Principle of heat transfer, 7th edition, pp. 322-324.

Phuong Thi Luu She received the B.S. degree in Electrical Engineering from Hanoi University of Science and Technology, Vietnam, in 2014. Currently she is studying as a Ph.D. student in integrative program in Korea Electrotechnology Research Institute (KERI) campus, which belongs to University of Science and Technology (UST). Her research interests are design and analysis of electromagnetic machines for transportation, robot, and medical systems.

Ji-Young Lee She received the B.S., M.S, and Ph.D. degrees in electrical engineering from Changwon National University, Korea, in 2000, 2002, and 2006 respectively. Now she is working as a senior researcher in Korea Electrotechnology Research Institute (KERI), and at the same time as an associate professor at University of Science & Technology (UST). Her research interests are design and analysis of electromagnetic machines for transportation, robot, and medical systems.

Ji-Won Kim He received the B.S. and M.S degrees in control & instrumentation engineering from University of Seoul, Korea in 1994 and Kwangwoon University, Korea in 1996 respectively. And Ph.D degree in electrical engineering from Pusan National University, Korea in 2014. Now he is working as a principal researcher in Korea Electrotechnology Research Institute (KERI), and at the same time as an associate professor at University of Science & Technology (UST). His research interests are industrial motor drive systems, electrical propulsion systems and tidal current generation systems.

Yon-Do Chun He received his B.S., M.S., and Ph.D. degrees in Electrical Engineering from Hanyang University in 1996, 1998, and 2001, respectively. From 2001 to 2003, he held a fellowship at the Japan Society for the Promotion of Science (JSPS), and he was with the Department of Electrical Engineering at Waseda University as a visiting scholar. From 2004 to 2012, he worked at the Korea Electrotechnology Research Institute (KERI). He is currently a chief researcher, Principal Researcher, at the Electric Motors Research Center, KERI and at the same time, an adjunct professor at University of Science & Technology (UST). His research interests are optimization design and analysis of various electric machines for the industrial applications.

Hong-Seok Oh He received the B.S., M.S, and Ph.D. degrees in electrical engineering from Yeungnam University, Korea, in 1992, 1994, and 2000 respectively. Now He is working as a managing director in Star Group Industry Company (SGI). His research interests are design and analysis of electromagnetic machines for transportation, and robot actuators.